AMERICAN SOCIETY FOR MICROBIOLOGY | Journal of Virology

Two Outbreak Sources of Influenza A (H7N9) Viruses Have Been Established in China

Dayan Wang, Lei Yang, Wenfei Zhu, Ye Zhang, Shumei Zou, Hong Bo, Rongbao Gao, Jie Dong, Weijuan Huang, Junfeng Guo, Zi Li, Xiang Zhao, Xiaodan Li, Li Xin, Jianfang Zhou, Tao Chen, Libo Dong, Hejiang Wei, Xiyan Li, Liqi Liu, Jing Tang, Yu Lan, Jing Yang, Yuelong Shu

National Institute for Viral Disease Control and Prevention, Collaboration Innovation Center for Diagnosis and Treatment of Infectious Diseases, Chinese Center for Disease Control and Prevention; Key Laboratory for Medical Virology, National Health and Family Planning Commission, Beijing, People's Republic of China

ABSTRACT

Due to enzootic infections in poultry and persistent human infections in China, influenza A (H7N9) virus has remained a public health threat. The Yangtze River Delta region, which is located in eastern China, is well recognized as the original source for H7N9 outbreaks. Based on the evolutionary analysis of H7N9 viruses from all three outbreak waves since 2013, we identified the Pearl River Delta region as an additional H7N9 outbreak source. H7N9 viruses are repeatedly introduced from these two sources to the other areas, and the persistent circulation of H7N9 viruses occurs in poultry, causing continuous outbreak waves. Poultry movements may contribute to the geographic expansion of the virus. In addition, the AnH1 genotype, which was predominant during wave 1, was replaced by JS537, JS18828, and AnH1887 genotypes during waves 2 and 3. The establishment of a new source and the continuous evolution of the virus hamper the elimination of H7N9 viruses, thus posing a long-term threat of H7N9 infection in humans. Therefore, both surveillance of H7N9 viruses in humans and poultry and supervision of poultry movements should be strengthened.

IMPORTANCE

Since its occurrence in humans in eastern China in spring 2013, the avian H7N9 viruses have been demonstrating the continuing pandemic threat posed by the current influenza ecosystem in China. As the viruses are silently circulated in poultry, with potentially severe outcomes in humans, H7N9 virus activity in humans in China is very important to understand. In this study, we identified a newly emerged H7N9 outbreak source in the Pearl River Delta region. Both sources in the Yangtze River Delta region and the Pearl River Delta region have been established and found to be responsible for the H7N9 outbreaks in mainland China.

Since the first emergence of influenza A (H7N9) virus in Eastern China (1), the novel virus has caused three outbreak waves in humans. The first outbreak emerged in late February 2013 and decreased rapidly after the middle of April 2013. The second wave began in October 2013, peaked in January 2014, and decreased in late February 2014. The number of H7N9 cases increased again in late 2014 and peaked in January 2015 during the third wave (Fig. 1A). By the end of September 2015, a total of 17 provinces or municipalities had been affected in Mainland China (Fig. 1), and 656 H7N9 cases had been reported, 268 of which were fatal. Imported cases were documented in Hong Kong SAR, in Taiwan, China, in Malaysia, and in Canada. Since October 2015, over 60 additional laboratory-confirmed cases of human infection with avian influenza A (H7N9) virus have been notified, indicating the beginning of the fourth outbreak wave.

Previous studies on the H7N9 virus have elucidated the potential origin and source of the virus (2–6). Dynamic reassortment among H7N9 and H9N2 viruses has been reported to increase the diversity of the virus (3–5, 7, 8). Frequent poultry movement and the silent spread of H7N9 viruses in poultry might have contributed to the H7N9 virus being enzootic in China (5). Several mammal-adapted mutations detected in H7N9 viruses have enhanced the threat of the novel virus in humans. It is important to monitor the virus evolution for pandemic preparedness. Hence, we conducted a panoramic molecular epidemiology study to analyze the three waves of H7N9 viruses.

MATERIALS AND METHODS

Virus isolation and subtyping. Fifty-three human H7N9 and avian origin H7N9 viruses have been previously sequenced (4). Between May 2013 and May 2015, a total of 232 H7N9 viruses were isolated from H7N9-positive human swabs ($n = 189$) or environmental samples ($n = 43$) confirmed by real-time PCR results in this study.

Virus isolation was conducted in a biosafety level 3 facility by inoculating 0.2-ml original samples allantoically into 9- to 11-day specific-pathogen-free (SPF) embryonated chicken eggs. After incubation at 37°C for 48 to 72 h, the allantoic fluids were harvested and tested for hemagglutinin (HA) agglutination by turkey red blood cells (TRBC). RNA was extracted for each virus using the RNeasy minikit (Qiagen, Hilden, Germany), and the subtype was further confirmed by sequencing.

Genome sequencing. Based on the real-time reverse transcription (RT)-PCR results, H7N9-positive RNAs were selected for Sanger se-

Received 17 December 2015 **Accepted** 18 March 2016

Accepted manuscript posted online 30 March 2016

Citation Wang D, Yang L, Zhu W, Zhang Y, Zou S, Bo H, Gao R, Dong J, Huang W, Guo J, Li Z, Zhao X, Li X, Xin L, Zhou J, Chen T, Dong L, Wei H, Li X, Liu L, Tang J, Lan Y, Yang J, Shu Y. 2016. Two outbreak sources of influenza A (H7N9) viruses have been established in China. J Virol 90:5561–5573. doi:10.1128/JVI.03173-15.

Editor: S. Schultz-Cherry, St Jude Children's Research Hospital

Address correspondence to Yuelong Shu, yshu@cnic.org.cn.

D.W., L.Y., W.Z., and Y.Z. contributed equally in this study.

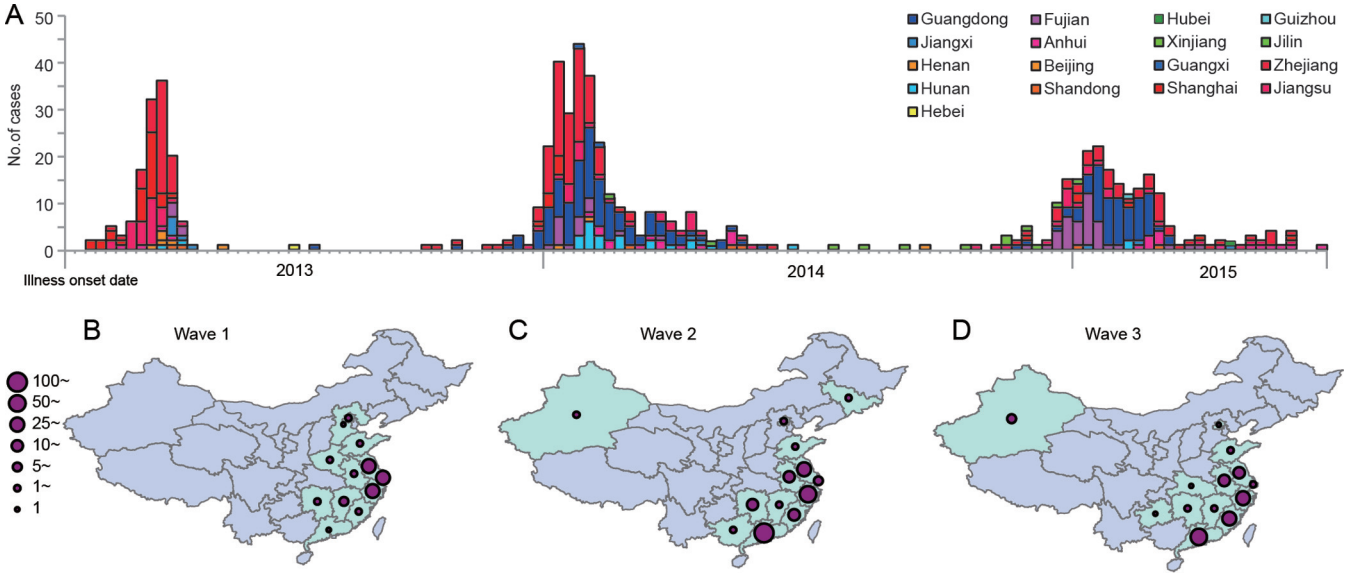

FIG 1 H7N9 case distribution from wave 1 to wave 3 in mainland China. From 9 Feb 2013 to 21 August 2015, a total of 656 H7N9 cases have been reported. (A) Epicurve of human H7N9 cases by date of illness onset. The cases were accumulated weekly. Colors indicate the H7N9-affected provinces. (B to D) H7N9 case distribution from the emergence of H7N9 to September 2013 (wave 1) (B), from October 2013 to July 2014 (wave 2) (C), and from October 2014 to August 2015 (wave 3) (D). H7N9-affected provinces are highlighted in light green. Solid violet circles vary from smallest to largest, indicating that the case number of H7N9 patients increased from 1 to >100.

quencing. Gene segments were amplified using the Qiagen OneStep RT-PCR kit. A total of 48 primer pairs were used to generate PCR amplicons among 378 and 1,123 bp in length for full-genome sequencing. Primer sequences are available from the authors on request. Amplified PCR products were purified using ExoSAP-IT reagent (USB, Cleveland, OH, USA). Complete genome sequencing was performed with an ABI 3730XL automatic DNA analyzer (Applied Biosystems, Foster City, CA, USA) using the ABI BigDye Terminator v3.1 cycle sequencing kit (Applied Biosystems), according to the manufacturer's recommendations.

Sequence alignment and phylogenetic analysis. The nucleotide sequences generated were assembled using Lasergene (Dnastar, Inc.) and combined with publicly available sequences of influenza A virus available in Global Initiative on Sharing All Influenza Data (GISAID) databases (http://www.gisaid.org). Reference sequences, which were phylogenetically related to the H7N9 viruses and had full-length sequences, were included with our sequences for phylogenic analysis.

A maximum likelihood phylogenetic tree for nucleotide sequences of each gene of selected influenza viruses was constructed under the GTRCAT model (a computational workaround for the general time-reversible model of nucleotide substitution under the Gamma model of rate heterogeneity) with 1,000 bootstrap replicates, using RAxML (9) via CIPRES Science Gateway (10). According to the bootstrap value and branch length, we classified each viral gene into clades. Combinations of the clades of all six internal genes of an isolate were defined as one genotype.

For BEAST analysis, virus sequences without sampling date information were excluded and the missing dates were set as the middle of month. According to the virus isolation locations, all sequences were classified into three regions as the Yangtze River Delta, the Pearl River Delta, and other regions.

The time-resolved Bayesian phylogenetic tree of HA gene was estimated by BEAST v1.8.2. The GTR + Gamma + Invariant substitution model was selected using jModelTest-2.1.4. The uncorrelated log-normal relaxed-clock model was employed to account for lineage-specific rate heterogeneity. The coalescent Bayesian sky grid model was used. Phylogeographic patterns were estimated using a symmetric continuous-time Markov chain (CTMC) model for discrete state reconstructions. The prior ucld.mean was set as uniform distribution. Markov chain Monte Carlo (MCMC) was run 3 times, each with 50 million steps sampled every 5,000 steps with burn-in of 5 million steps and samples combined. The effective sample size (ESS) of all priors was greater than 200. The migration rates were calculated using posterior analysis of coalescent trees (PACT) from Github.

Nucleotide sequence accession numbers. Full-genome sequences of 232 H7N9 viruses in our study have been deposited into GISAID with the accession numbers EPI626978 to EPI628832.

RESULTS

Evolutionary relationships of hemagglutinin genes of H7N9 viruses during waves 1 to 3. Based on both RAxML and BEAST analyses of the H7 hemagglutinin (HA) genes (Fig. 2 and 3), all viruses from all affected regions in wave 1 clustered into one group and originated exclusively from the Yangtze River Delta region. This result further supported that the Yangtze River Delta region was the source responsible for the wave 1 H7N9 outbreak (4). In contrast to wave 1, the HA gene of wave 2 viruses clustered into 6 clades (W2-1, W2-2, W2-3, W2-4, W2-5, and W2-6 [Fig. 2A]). All outgroup viruses of these six clades were detected from wave 1, indicating that all H7N9 viruses of wave 2 originated exclusively from wave 1. In each clade, H7N9 viruses of human and avian origins shared numerous similarities and clustered together (Fig. 2D), further verifying the avian-to-human transmission of influenza A (H7N9) viruses.

Clade W2-1 included primarily viruses isolated in the Pearl River Delta region, including Guangdong province and Hong Kong SAR, China (Fig. 2B and C). In agreement with a previous study (5), clade W2-1 includes a large number of H7N9 viruses of both human and avian origins, suggesting that influenza A (H7N9) viruses may have become established in poultry during the second wave (Fig. 2D). Thus, the establishment of H7N9 in poultry caused the large number of human infections in wave 2 in

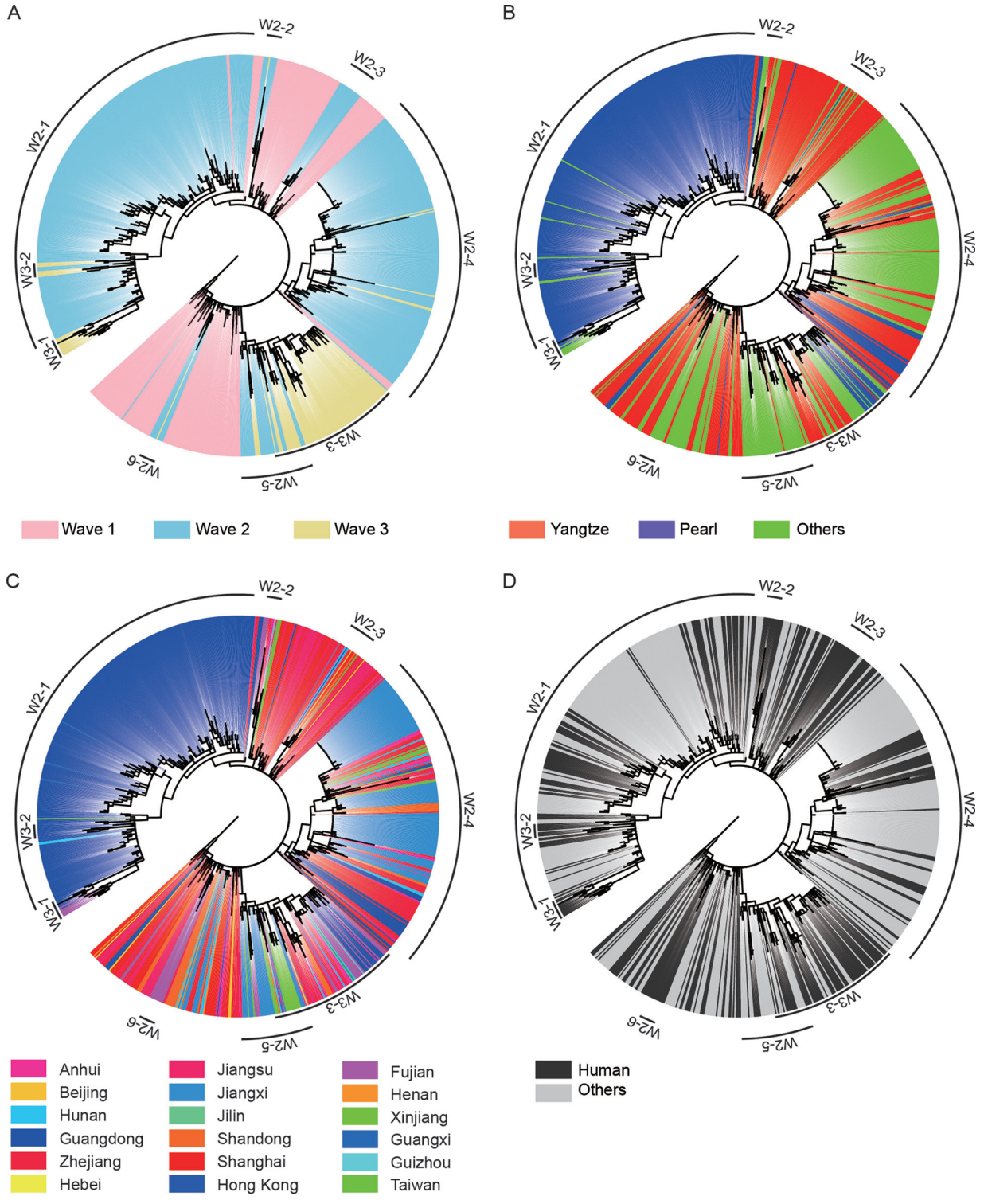

FIG 2 Phylogenetic trees of HA genes of influenza A (H7N9) viruses from wave 1 to wave 3 estimated using RAxML. Trees are presented in a circular format with the same topology in all panels. (A) H7N9 viruses collected during the first wave are highlighted with the background shading in pink, and those during the second and third waves are in light blue and light yellow, respectively. (B) H7N9 viruses isolated from the Yangtze River Delta regions, the Pearl River Delta regions, and other regions are shown in red, blue, and green, respectively. (C) Different colors indicate the provinces from which the corresponding H7N9 viruses came. (D) Black or gray denote the human or nonhuman H7N9 viruses, respectively. Reference viruses representing each subclade are listed in Table 7.

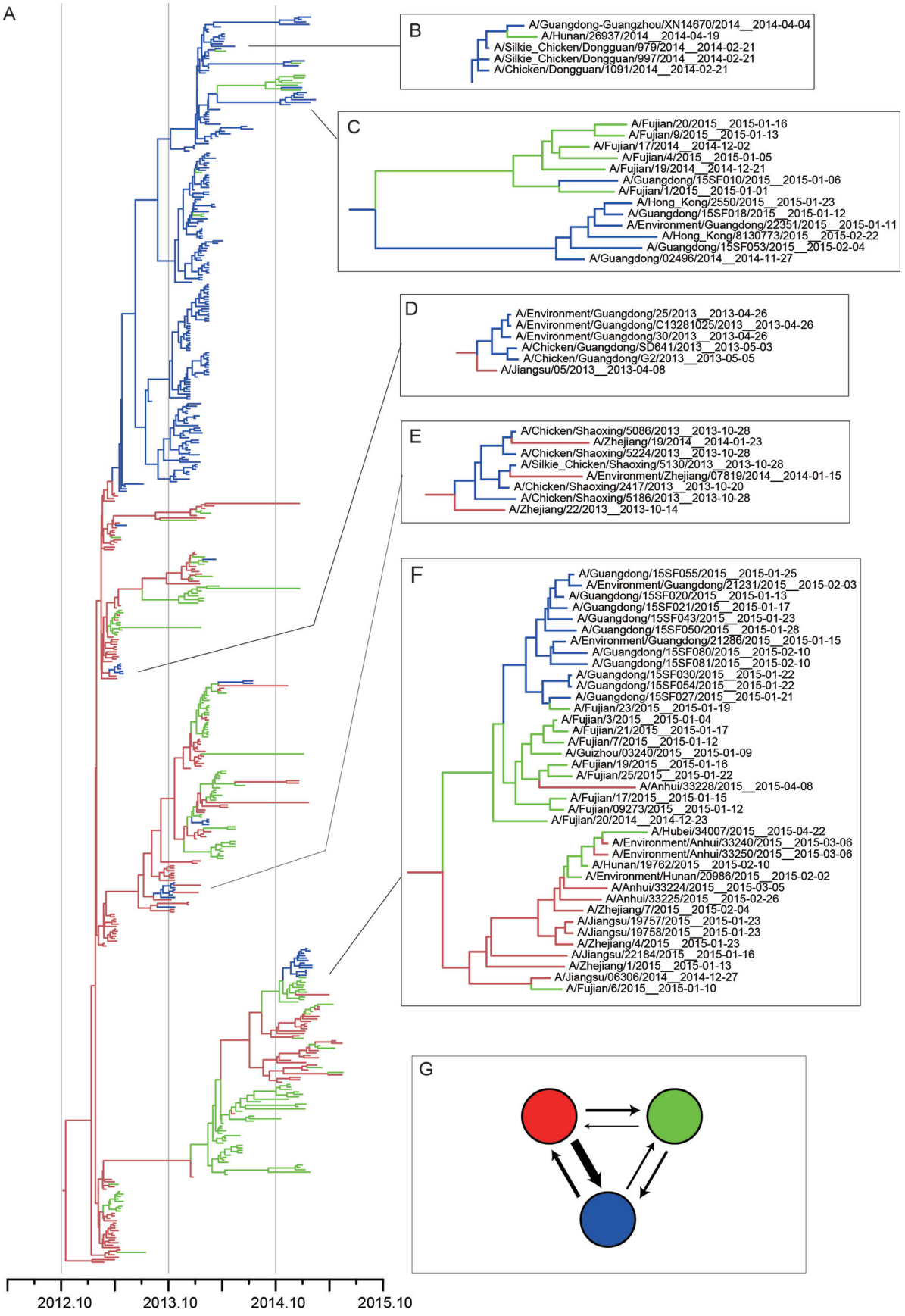
A
B
A/Guangdong-Guangzhou/XN14670/2014__2014-04-04
A/Hunan/26937/2014__2014-04-19
A/Silkie_Chicken/Dongguan/979/2014__2014-02-21
A/Silkie_Chicken/Dongguan/997/2014__2014-02-21
A/Chicken/Dongguan/1091/2014__2014-02-21
C
A/Fujian/20/2015__2015-01-16
A/Fujian/9/2015__2015-01-13
A/Fujian/17/2014__2014-12-02
A/Fujian/4/2015__2015-01-05
A/Fujian/19/2014__2014-12-21
A/Guangdong/15SF010/2015__2015-01-06
A/Fujian/1/2015__2015-01-01
A/Hong_Kong/2550/2015__2015-01-23
A/Guangdong/15SF018/2015__2015-01-12
A/Environment/Guangdong/22351/2015__2015-01-11
A/Hong_Kong/8130773/2015__2015-02-22
A/Guangdong/15SF053/2015__2015-02-04
A/Guangdong/02496/2014__2014-11-27
D
A/Environment/Guangdong/25/2013__2013-04-26
A/Environment/Guangdong/C13281025/2013__2013-04-26
A/Environment/Guangdong/30/2013__2013-04-26
A/Chicken/Guangdong/SD641/2013__2013-05-03
A/Chicken/Guangdong/G2/2013__2013-05-05
A/Jiangsu/05/2013__2013-04-08
E
A/Chicken/Shaoxing/5086/2013__2013-10-28
A/Zhejiang/19/2014__2014-01-23
A/Chicken/Shaoxing/5224/2013__2013-10-28
A/Silkie_Chicken/Shaoxing/5130/2013__2013-10-28
A/Environment/Zhejiang/07819/2014__2014-01-15
A/Chicken/Shaoxing/2417/2013__2013-10-20
A/Chicken/Shaoxing/5186/2013__2013-10-28
A/Zhejiang/22/2013__2013-10-14
F
A/Guangdong/15SF055/2015__2015-01-25
A/Environment/Guangdong/21231/2015__2015-02-03
A/Guangdong/15SF020/2015__2015-01-13
A/Guangdong/15SF021/2015__2015-01-17
A/Guangdong/15SF043/2015__2015-01-23
A/Guangdong/15SF050/2015__2015-01-28
A/Environment/Guangdong/21286/2015__2015-01-15
A/Guangdong/15SF080/2015__2015-02-10
A/Guangdong/15SF081/2015__2015-02-10
A/Guangdong/15SF030/2015__2015-01-22
A/Guangdong/15SF054/2015__2015-01-22
A/Guangdong/15SF027/2015__2015-01-21
A/Fujian/23/2015__2015-01-19
A/Fujian/3/2015__2015-01-04
A/Fujian/21/2015__2015-01-17
A/Fujian/7/2015__2015-01-12
A/Guizhou/03240/2015__2015-01-09
A/Fujian/19/2015__2015-01-16
A/Fujian/25/2015__2015-01-22
A/Anhui/33228/2015__2015-04-08
A/Fujian/17/2015__2015-01-15
A/Fujian/09273/2015__2015-01-12
A/Fujian/20/2014__2014-12-23
A/Hubei/34007/2015__2015-04-22
A/Environment/Anhui/33240/2015__2015-03-06
A/Environment/Anhui/33250/2015__2015-03-06
A/Hunan/19762/2015__2015-02-10
A/Environment/Hunan/20986/2015__2015-02-02
A/Anhui/33224/2015__2015-03-05
A/Anhui/33225/2015__2015-02-26
A/Zhejiang/7/2015__2015-02-04
A/Jiangsu/19757/2015__2015-01-23
A/Jiangsu/19758/2015__2015-01-23
A/Zhejiang/4/2015__2015-01-23
A/Jiangsu/22184/2015__2015-01-16
A/Zhejiang/1/2015__2015-01-13
A/Jiangsu/06306/2014__2014-12-27
A/Fujian/6/2015__2015-01-10
G
2012.10
2013.10
2014.10
2015.10

this area. As shown in Fig. 2B and C, clade W2-1 viruses originated from the Yangtze River region and persisted in Guangdong Province. Some viruses of this clade spread to the Guangxi and Hunan provinces, indicating that another potential source in the Pearl River Delta region readily emerged during wave 2.

Viruses of other clades of wave 2 (W2-2, W2-3, W2-4, W2-5, and W2-6) contain viruses detected in multiple provinces, especially W2-4 and W2-5 (Fig. 2C). Human isolates from Jilin and Xinjiang, which are geographically far away from eastern China, involved clades W2-4 and W2-5, respectively. Outgroup viruses of these two clades were detected exclusively in the Yangtze River region (Fig. 2B). This result indicated that viruses of these clades may have originated and spread from the Yangtze River region to other regions. In addition, several viruses in clade W2-4 were isolated from Guangdong (Fig. 2B and 3E), suggesting the repeated introduction of H7N9 viruses from the Yangtze River region to the Pearl River Delta region.

The majority of viruses from wave 3 were clustered into three clades (W3-1, W3-2, and W3-3) (Fig. 2). The viruses of wave 3 were descended exclusively from the viruses of wave 2. Among the viruses, W3-1 and W3-2 viruses circulated primarily in Guangdong and originated from viruses of W2-1, indicating that the virus historically circulating in Guangdong during wave 2 was persistent in this area during wave 3. More importantly, viruses isolated from Fujian Province clustered into clade W3-1 (Fig. 2C and 3C), further supporting the notion that the Pearl River Delta region was an additional source of H7N9 outbreaks. W3-3 viruses that originated from W2-5 constituted the primary circulated cluster during wave 3. It contained viruses circulated in the Yangtze River Delta region and in Guangdong, providing evidence on the introduction of genes from the Yangtze River Delta region to the Pearl River Delta region (Fig. 2 and 3). Besides, clade W3-3 viruses caused human infections both in the Yangtze River Delta region and in other provinces, including northwestern and southeastern China (Fig. 2). This result strongly supports the contention that the Yangtze River Delta region was an important source for H7N9 outbreaks.

Evolutionary relationships of NA gene and six internal genes of H7N9 viruses during waves 1 to 3. As shown in Fig. 4A, the phylogenetic tree of the neuraminidase (NA) gene (N9) exhibited a topology similar to that of the HA tree, with the wave 2 viruses divided into 6 corresponding clades and wave 3 viruses separated into 3 clades. Of note, six human H7N9 viruses isolated from the Fujian province [A/Fujian/1/2015(H7N9) and others] in wave 3 had HA genes descended from viruses detected in Guangdong (clade W3-1) and the NA genes grouped into clade W3-3, indicating that the H7N9 viruses were transmitted from Guangdong to Fujian and generated new variants.

Six internal genes of all H7N9 viruses studied were broadly classified into multiple clades. The PB2 and PB1 genes were divided into four major clades, and the NP and M genes were divided into three clades. For the PA and NS genes, two major clades were clustered (Fig. 4B).

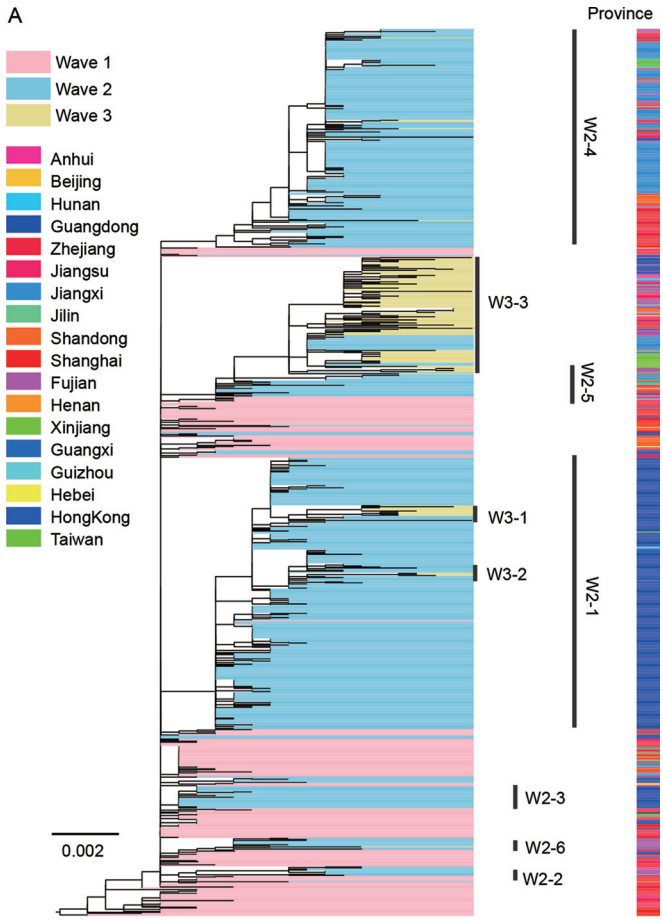

FIG 4 Evolution of NA (A) and six internal genes (B) of influenza A (H7N9) viruses from wave 1 to wave 3. RAxML was used to estimate the phylogenetic relationships. In the phylogenetic tree, H7N9 viruses collected during the first wave are highlighted with the background shading in pink, and those during the second and third waves are in light blue and light yellow, respectively. Colors in the right side of panel A indicate the provinces from which the corresponding H7N9 viruses came.

Classification of H7N9 genotypes during waves 1 to 3. Based on different clade combinations of 6 internal genes, at least 93 genotypes were identified (Fig. 5). Most of the genotypes (83/93) were circulated only transiently. During wave 1, AnH1, JS1, and SH7 genotype viruses were the predominant viruses, while in wave 2, JS537, which was detected only once during wave 1, rapidly became a dominant H7N9 virus genotype. In addition, another six genotypes (JS18828, AnH1887, GD1, GD10, GD2, and GD429) were cocirculated as well; however, only two

FIG 3 Bayesian maximum clade credibility (MCC) phylogeny of H7 gene sequences of wave 1 to wave 3. All viruses isolated in the Yangtze River Delta region, the Pearl River Delta region, and other regions are highlighted in red, blue, and green, respectively. (A) BEAST tree of the H7N9 viruses estimated using the HA gene sequences. (B and C) Representative clades showing virus expansion from the Pearl River Delta region to other regions. (D and E) Representative clades showing virus expansion from the Yangtze River Delta region to the Pearl River Delta region. (F) Representative clades showing virus expansion from the Yangtze River Delta region to the Pearl River Delta region or other regions. (G) Virus migration rate among the Yangtze River Delta region, the Pearl River Delta region, and other regions. Colors in the solid circles correspond to the regions shown in the phylogenetic tree. Thicker arrows indicate the higher migration rate between two indicated regions. The migration rates were calculated using PACT.

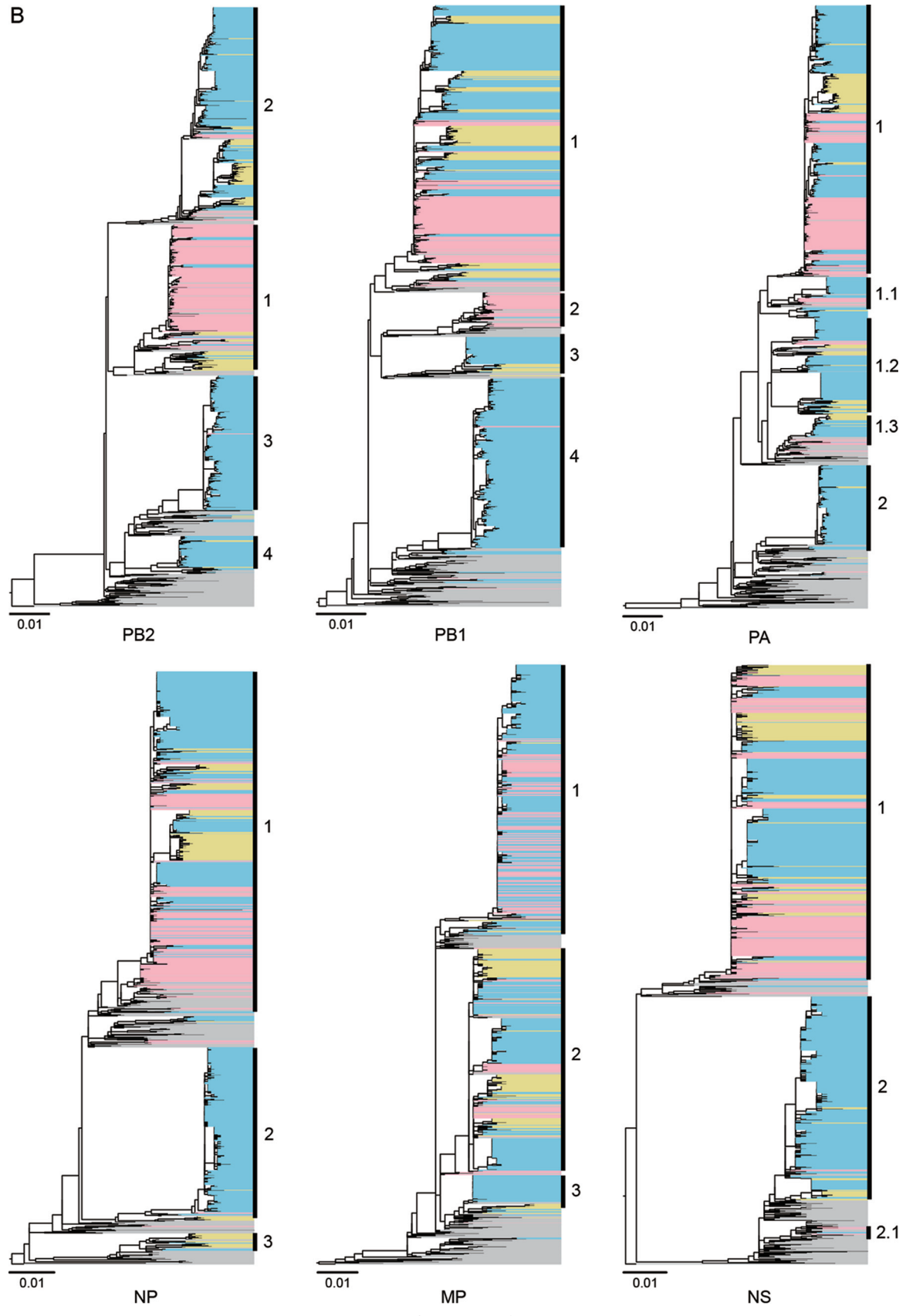

FIG 4 continued

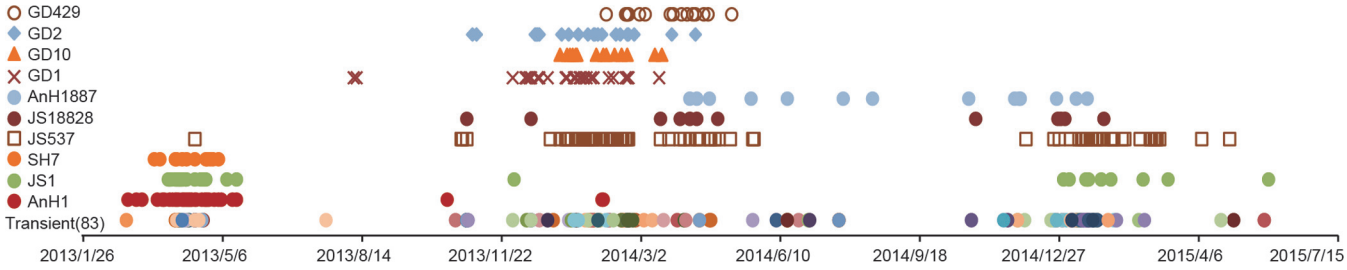

FIG 5 Timeline of influenza A (H7N9) virus genotypes during three outbreak waves. Ten predominant genotypes (GD429, GD2, GD10, GD1, AnH1887, JS18828, JS537, SH7, JS1, and AnH1) are listed on the left. All 83 transient genotypes are on the bottom line. Symbols represent the corresponding genotypes of H7N9 viruses and their time of isolation.

AnH1 viruses and one JS1 virus were detected during the early stage of wave 2. During wave 3, four genotypes, including JS18828, AnH1887, JS537, and JS1, were persistent from wave 2. Another 4 genotypes (GD1, GD10, GD2, and GD429), which dominated in wave 2, on the other hand, were not detected during this period.

Formation and establishment of two outbreak sources of H7N9 viruses. The genotype geographical distribution data identified the Pearl River Delta region as the subsource of H7N9 viruses, which were generated from the Yangtze River Delta region (Fig. 6). Six dominant genotypes, including AnH1, JS1, SH7, JS537, JS18828, and AnH1887, were generated in the Yangtze River Delta region and responsible for the majority of cases in other affected regions. Genotypes AnH1, JS1, JS537, and JS18828 were introduced into the Pearl River Delta region. Genotypes GD1, GD10, GD2, and GD429, which were generated by reassortment with local H9N2 viruses (11), circulated mainly in Guangdong Province. Genotypes GD1 and GD10 further spread to Guangxi Province and genotype GD429 to Hunan Province. Because the AnH1 genotype disappeared rapidly after wave 2 and JS537 genotype viruses were detected widely and persistently during all three waves, we speculated that JS537 might have replaced AnH1 genotype and become the predominant circulated genotype.

As shown in Fig. 1B to D, the geographic distribution of H7N9 cases further supported the two sources of H7N9 outbreaks. During wave 1, the majority of H7N9 cases were distributed in the Yangtze River Delta region, including Jiangsu, Shanghai, and Zhejiang Provinces (Fig. 1A and B and Table 1). The H7N9 virus from the Yangtze River Delta region was introduced into Guangdong Province and caused the first human infection in Huizhou City at the end of wave 1 (early August 2013 [12]) (Fig. 1B). During waves

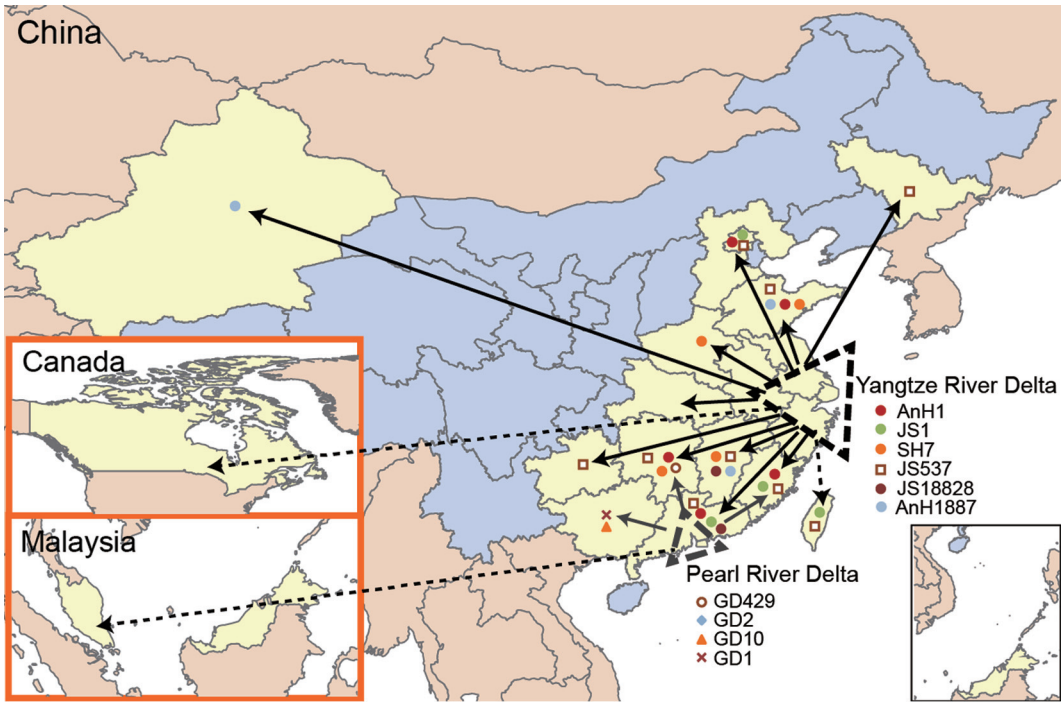

FIG 6 Genotype flow of the influenza A (H7N9) viruses. All H7N9-affected regions are highlighted in light yellow. Two H7N9 sources, the Yangtze River Delta and the Pearl River Delta regions, are highlighted with larger and smaller dotted black triangles, respectively. Dominant genotypes in each source are listed below the corresponding triangles. Virus spreads are indicated by solid arrows. The dotted arrows indicate that the imported H7N9 cases occurred in Taiwan, China, in Malaysia, or in Canada.

TABLE 1 Geographic distribution of influenza A (H7N9) cases during the three waves

Region and province or city	No. of cases			
	First wave	Second wave	Third wave	Total
Yangtze River Delta	136	61	22	219
Zhejiang	41	46	14	101
Jiangsu	48	8	8	64
Shanghai	47	7		54
Pearl River Delta	16	297	28	341
Guangdong	16	286	25	327
Hongkong		11	3	14
Other regions	44	191	63	298
Jiangxi	8	126		134
Fujian	3	16	27	46
Anhui	5	12	11	28
Shandong	13	10	5	28
Hunan	4	9	5	18
Beijing	4	1	1	6
Henan	3			3
Hebei	1			1
Guangxi		3	1	4
Guizhou		1	1	2
Xinjiang		3	11	14
Jilin		7		7
Hubei			1	1

TABLE 2 Posterior estimate of migration rates between regions[a]

Statistic	Posterior migration rate mean (95% interval)
YRD to PRD	0.26 (0.16, 0.38)
YRD to OR	0.94 (0.71, 1.2)
PRD to YRD	0.11 (0.05, 0.2)
PRD to OR	0.25 (0.19, 0.34)
OR to YRD	0.38 (0.19, 0.62)
OR to PRD	0.22 (0.12, 0.35)

[a] The migration rate is calculated as migration events per lineage per year between two regions, using PACT. Abbreviations: YRD, Yangtze River Delta; PRD, Pearl River Delta; OR, other region.

2 and 3, the H7N9 viruses were persistent and continually reassorted their six internal genes with local H9N2 viruses circulating in poultry in the Pearl River region. The progeny H7N9 viruses were disseminated to the neighbor provinces, such as Guangxi, Hunan, and Fujian Provinces. Supported by the distribution and expansion of H7N9 viruses, human cases in Guangdong increased and the largest numbers of H7N9 cases were reported in the same province during wave 2, followed by Zhejiang and Jiangsu Provinces (Fig. 1C and Table 1). Moreover, the majority of H7N9 cases were distributed along the southeastern coastal line provinces in wave 3, covering both the Yangtze River Delta and Pearl River Delta regions (Fig. 1D and Table 1). The Yangtze River Delta region persistently acted as the main source during all three waves and was responsible for the H7N9 cases in most affected regions, limited not only to the neighboring provinces but also to the distant provinces, such as Xinjiang in northwestern China and Jilin in northern China (Fig. 1B to D).

We further calculated the migration rates among the Yangtze River Delta region, the Pearl River Delta region, and the other regions. As shown in Fig. 3G and in Table 2, the migration rate from Yangtze River Delta region to other regions was the highest (mean, 0.94), further supporting the Yangtze River Delta region as the major H7N9 outbreak source. Besides, the migration rate from the Pearl River Delta region to the other regions is 0.25, indicating this region as another potential H7N9 outbreak source.

Host adaption mutations and antigenic characterization during waves 1 to 3. Given the wide distributions of the viruses and the frequent reassortment among H7N9 and H9N2 viruses, we further analyzed the amino acid mutations associated with mammalian adaptation and antiviral drug resistance. The results are summarized in Table 3.

For the HA gene, most viruses contained G186V and Q226L/I substitutions (H3 numbering), increasing the human receptor binding of the viruses (13–16). During the three waves, a reduced number of human H7N9 viruses retained the residue with 186G or 226Q. The majority of human origin H7N9 viruses of each wave acquired PB2-E627K, which increased viral pathogenicity in mice (17–19). Of note, almost all of the human- or avian-origin H7N9 viruses possessed the I368V mutation in PB1 protein, which would increase the H5N1 viral transmissibility in ferrets (20). A total of 5.4% (19/352) of the H7N9 viruses possessed substitutions associated with drug resistance in the NA protein, indicating the sensitivity of neuraminidase inhibitors. More specifically, a total of 4, 1, and 14 human-origin H7N9 viruses possessed either E119V, A246T, or R292K substitutions in NA protein, respectively (21). None of the mutations occurred in avian-origin H7N9 viruses. All H7N9 viruses were resistant to adamantine due to the S31N mutation in M2 protein (1, 16, 22).

Hemagglutinin inhibition assays were conducted on the selected viruses representing each subclade of all three waves according to standard protocols using 0.5% turkey red blood cells (23, 24). The results showed that all H7N9 viruses reacted well with the antisera of the vaccine virus A/Anhui/1/2013 (Tables 4, 5, and 6). No antigenic differences were observed.

DISCUSSION

Due to the asymptomatic infections of H7N9 viruses in poultry (25–27), humans acted as the sentinels for the presence of these viruses in avian infections. After three outbreak waves, the fourth epidemic is ongoing. In view of influenza pandemic preparedness, H7N9 activities of the past three waves in humans in China are very important to understand. Thus, genomic, epidemic, and antigenic analyses of the three waves of H7N9 viruses were conducted in this study.

The results have shown that two H7N9 sources have been established in China (Fig. 6). The larger one is the Yangtze River Delta region, which is well recognized as the original source of the H7N9 outbreaks, and the other is the Pearl River Delta region, where viruses also originated from the Yangtze River Delta region. Multiple introductions of the viruses from the Yangtze Delta region into the Pearl River region and the spread of the virus from these two sources to other regions resulted in the virus expansion and human infections.

Several contributions may facilitate the Pearl River Delta region as the subsource of H7N9 outbreaks. The extensive and semi-intensive poultry production systems and live poultry markets in

TABLE 3 Key amino acid substitutions of influenza A (H7N9) viruses during the three waves[a]

Gene	Function	Mutation	Amino acid	First wave	Second wave	Third wave	Nonhuman isolate
HA	Altered receptor specificity	A160S/T	A	97	166	92	490
			S/T	1	3	0	0
	Favor mammalian adaptation, Receptor binding site	G186V	G	3	0	0	0
			V	95	170	84	487
			A	0	0	8	3
		Q226L/I	Q	5	1	0	20
			L	87	168	84	460
			I	5	0	7	5
			S	0	1	1	1
			P	1	0	0	0
NA	Related to drug resistance	E119V	E	91	163	92	488
			V	1	3	0	0
		R292K	R	86	160	92	488
			K	6	6	0	0
PB2	Mammalian host adaptation	D256G	D	91	160	90	476
			G	1	0	1	0
	Enhance the 627K and 701N function	K526R	K	84	159	89	474
			R	8	1	2	2
	Altered replication efficiency and virulence in mice	Q591K	Q	86	152	87	475
			K	4	4	3	1
			L	0	3	0	0
	Increased virulence in mice	E627K	E	29	32	32	475
			K	62	122	52	1
			Q	0	0	1	0
			V	0	2	2	0
	Enhanced transmission in guinea pigs	D701N	D	83	146	88	474
			N	8	14	3	1
	Species-associated signature positions	K702R	K	92	157	91	473
			R	0	3	0	3
PB1	Increased transmission in ferret	I368V	I	11	0	0	6
			V	75	161	92	467
	Increased replication in mammalian cells	L598P	L	85	162	91	473
			Q	0	0	1	0
			M	1	0	0	0
PB1-F2	Increased pathogenicity in mice	87–90 amino acids in length	11AA	1	0	0	0
			25AA	11	1	0	24
			27AA	0	0	1	0
			34AA	0	0	11	45
			57AA	0	17	0	35
			76AA	3	0	1	13
			79AA	0	0	1	0
			90AA	71	144	76	355
			101AA	0	0	1	0
	Altered virulence and antivirus response in mice	N66S	N	86	162	92	473
			S	0	2	0	0
PA	Species-associated signature positions	V100A	V	9	55	35	261
			A	77	87	55	202
			I	0	21	2	2
			T	0	0	0	1
	Increase the polymerase activity in mice	L336M	L	86	129	90	368
			M	0	34	2	98
	Species-associated signature positions	K356R	K	0	35	2	99
			R	86	128	90	367
		S409N	S	6	12	7	60
			N	80	151	85	406

(Continued on following page)

TABLE 3 (Continued)

Gene	Function	Mutation	Amino acid	First wave	Second wave	Third wave	Nonhuman isolate
NS1	Altered virulence in mice	D92E	D	89	164	92	476
			E	2	0	0	0
	Altered antiviral response in host	N205S	N	0	3	0	6
			S	91	161	90	464
			C	0	0	0	5
			R	0	0	2	1
		G210R	G	91	164	92	472
			R	0	0	0	4

[a] Values indicate the number of isolates with the given mutation. Identical molecular markers that exist in all influenza A (H7N9) virus isolates and have been reported to have functions in other influenza virus subtypes are not listed in this table. They include the following: PB2 (89V and 357H, indicating increased pathology in mice), PB1 (473V, indicating increased replication in mammalian cells), PA (36A, reported to be related to increased replication), M1 (30D and 215A, related to increased virulence in mice), M2 (31N, indicating reduced sensitivity to amantadine), NS1 (42S, indicating increased virulence in mice; PDZ motif deletion, indicating decreased virulence in mice). Mixed residues are not included for analysis. The HA gene was under the H3 numbering system and the NA gene under the N2 numbering system. Other internal genes were numbered from the start codon (M).

TABLE 4 Hemagglutination inhibition reactions of influenza H7N9 viruses in experiments conducted on 15 February 2016[a]

Isolate no.	Virus description	Titer			Passage history	Collection date (yr-mo-day)	Phylogenetic clade
		HA	AH1	SH2			
1	A/Anhui/1/2013 (reference)	256	**160**	320	E2	2013-03-20	W1
2	A/Shanghai/2/2013 (reference)	64	160	**320**	E2	2013-03-05	W1
3	A/Guangdong/24997/2013	1,024	320	320	E1	2013-11-30	W2-1
4	A/Guangdong/24999/2013	128	160	320	E1	2013-12-16	W2-1
5	A/Guangdong/02125/2014	128	160	320	E1	2014-01-08	W2-1
6	A/Guangdong-Guangzhou/XN00509/2014	512	320	320	E1	2014-02-10	W2-1
7	A/Guangdong-Guangzhou/XN08763/2014	256	160	160	E1	2014-02-21	W2-1
8	A/Shandong/02/2014	512	160	320	E1	2014-03-04	W2-3
9	A/Jiangsu/09041/2014	512	160	320	E1	2014-01-20	W2-3
10	A/Guangdong/15SF017/2015	64	160	320	E1	2015-01-15	W3-2
11	A/Jiangsu/19758/2015	512	160	160	E1	2015-01-23	W3-3
12	A/Jiangsu/18828/2014	256	80	80	E1	2014-12-31	W3-3
13	A/Anhui/01887/2014	64	80	80	E1	2014-05-20	W3-3
14	A/Anhui/33228/2015	128	160	160	E1	2015-04-08	W3-3
15	A/Beijing/40610/2015	64	80	80	E1	2015-05-26	W3-3
16	A/Anhui/40095/2015	64	80	160	E1	2015-05-23	W3-3
17	A/Guangdong/15SF010/2015	512	160	320	E1	2015-01-06	W3-1
18	A/Environment/Guangdong/22351/2015	1,024	80	160	E1	2015-01-11	W3-1
19	A/Environment/Guangdong/21123/2015	256	160	320	E1	2015-01-20	W3-1

[a] In Tables 4 to 6, the virus description gives the type/region/strain number/year of isolation. The first two are reference strains, and the rest are test strains. Values in boldface indicate homologous titers of reference viruses.

TABLE 5 Hemagglutination inhibition reactions of influenza H7N9 viruses in experiments conducted on 15 August 2014

Isolate no.	Virus description	Titer			Passage history	Collection date (yr-mo-day)	Phylogenetic clade
		HA	AH1	SH2			
1	A/Anhui/1/2013 (reference)	256	**160**	640	E2	2013-03-20	W1
2	A/Shanghai/2/2013 (reference)	512	160	**640**	E1	2013-03-05	W1
3	A/Fujian/16/2014	512	160	1,280	E1	2014-03-28	W2-6
4	A/Zhejiang/24/2014	1,024	320	1,280	E1	2014-01-24	W2-4
5	A/Zhejiang/23/2014	512	320	1,280	E1	2014-02-09	W2-4
6	A/Zhejiang/22/2014	512	80	640	E1	2014-02-08	W2-4
7	A/Zhejiang/21/2014	128	160	1,280	E1	2014-02-10	W2-4
8	A/Zhejiang/20/2014	128	160	1,280	E1	2014-02-03	W2-4
9	A/Zhejiang/17/2014	4,096	80	640	E1	2014-02-03	W2-4
10	A/Zhejiang/16/2014	4,096	160	320	E1	2014-02-03	W2-4
11	A/Zhejiang/15/2014	256	320	1,280	E1	2014-01-25	W2-4
12	A/Zhejiang/14/2014	512	160	640	E1	2014-01-14	W2-4
13	A/Zhejiang/13/2014	512	160	640	E1	2014-01-27	W2-3
14	A/Fujian/15/2014	64	160	640	E1	2014-02-26	W2-2
15	A/Jiangxi/27569/2014	512	160	1,280	E1	2014/4/21	W2-4
16	A/Hunan/26937/2014	256	160	640	E1	2014/4/19	W2-1
17	A/Hunan/26938/2014	256	80	640	E1	2014/4/19	W2-1
18	A/Environment/Xinjiang/73033/2014	128	80	80	E1	2014/7/25	W2-5

TABLE 6 Hemagglutination inhibition reactions of influenza H7N9 viruses in experiments conducted on 17 June 2013

Isolate no.	Virus description	Titer			Passage history	Collection date (yr-mo-day)	Phylogenetic clade
		HA	AH1	SH2			
1	A/Anhui/1/2013 (reference)	16	**320**	640	E1	2013-03-20	W1
2	A/Shanghai/2/2013 (reference)	256	320	**640**	E1	2013-03-05	W1
3	A/Shanghai/1/2013	256	160	320	E2	2013-02-26	W1
4	A/Shanghai/3/2013	256	320	640	E1	2013-02-27	W1
5	A/Shanghai/4/2013	512	320	640	E2	2013-03-09	W1
6	A/Jiangsu/01/2013	64	320	640	E2	2013-03-30	W1
7	A/Zhejiang/01/2013	512	320	640	E1	2013-03-25	W1
8	A/Shanghai/05/2013	1,024	80	160	E1	2013-04-02	W1
9	A/Shanghai/07/2013	128	640	1,280	C2	2013-03-18	W1
10	A/Jiangsu/02/2013	64	320	1,280	E1	2013-03-31	W1
11	A/Jiangsu/03/2013	1,024	320	640	E1	2013-04-06	W1
12	A/Jiangsu/04/2013	512	160	320	E1	2013-04-05	W1
13	A/Beijing/01-A/2013	512	320	640	E1	2013-04-12	W1
14	A/Shanghai/06-A/2013	256	320	640	E1	2013-04-10	W1
15	A/Shanghai/10/2013	512	640	1,280	E1	2013-04-09	W1
16	A/Shanghai/11/2013	128	320	640	E1	2013-04-10	W1
17	A/Shanghai/12/2013	256	640	1,280	E1	2013-04-10	W1
18	A/Shanghai/13/2013	32	160	320	E1	2013-04-10	W1
19	A/Shanghai/14/2013	1,024	640	1,280	E1	2013-04-10	W1
20	A/Shanghai/17/2013	512	160	640	E1	2013-04-03	W1
21	A/Shanghai/8/2013	32	320	1,280	E1	2013-04-07	W1
22	A/Shanghai/9/2013	256	320	640	E1	2013-04-08	W1
23	A/Zhejiang/02/2013	128	320	640	E1	2013-04-03	W1
24	A/Shanghai/15/2013	128	320	640	E2	2013-04-09	W1
25	A/Shanghai/16/2013	512	640	1,280	E2	2013-04-10	W1
26	A/Henan/01/2013	12	160	320	E1	2013-04-16	W1
27	A/Shandong/01/2013	256	320	640	E1	2013-04-21	W1
28	A/Fujian/01/2013	512	320	640	E1	2013-04-23	W1
29	A/Jiangxi/01/2013	128	320	640	E1	2013-04-24	W1
30	A/Hunan/01/2013	256	160	640	E1	2013-04-24	W1
31	A/Hunan/02/2013	128	320	640	E1	2013-04-25	W1
32	A/Jiangsu/05/2013	512	160	640	E1	2013-04-08	W1
33	A/Jiangsu/06/2013	128	320	640	E1	2013-04-10	W1
34	A/Jiangsu/07/2013	512	320	640	E1	2013-04-03	W1
35	A/Jiangsu/08/2013	512	640	1,280	E1	2013-04-11	W1
36	A/Jiangsu/09/2013	512	320	640	E1	2013-04-09	W1
37	A/Anhui/02/2013	512	320	1,280	E1	2013-04-14	W1
38	A/Anhui/03/2013	64	640	1,280	E1	2013-04-21	W1
42	A/Chicken/Anhui-Chuzhou/01/2013	512	320	1,280	E1	2013-03-29	W1
43	A/Environment/Shandong/1/2013	128	320	640	E1	2013-04-27	W1

the Pearl River Delta region resulted in the fact that multiple species of poultry shared the same environment (28). A large diversity of avian influenza subtypes, including H5N1 and H9N2 subtype viruses, have been identified from both wild and domestic birds in the Pearl River Delta region (29–31). These may benefit the reassortment of H7N9 viruses with local avian influenza viruses (11, 32) and enhance the opportunity for the genesis and transmission of different genotypes of H7N9 viruses. Moreover, poultry movements could increase opportunities for the spread of the virus from this contaminated region to other regions.

Our results have shown that the H7N9 viruses generated in the Yangtze River Delta or Pearl River Delta region could spread to other regions in Mainland China, including Xinjiang and Jilin, which were distant from these sources but in which human infections still occurred. The poultry trade or movement of poultry may contribute to the geographic expansion of H7N9 viruses, thereby increasing the risk of the H7N9 viruses crossing the border and spreading to other regions or countries. Regional expansion of H7N9 viruses increased the possibilities of reassortment among H7N9 and other subtype viruses. Furthermore, the accumulation proportion of the mammal-adapted substitutions, such as substitutions occurring in position 186 or 226 in HA protein, could increase the likelihood of the viral interspecies transmission. Therefore, these two regions should be monitored to control any H7N9 outbreaks, and the following should be encouraged: relocation of the poultry productions systems away from live poultry markets, raising of the biosecurity level in farms and markets, closure of live poultry markets, active surveillance in humans and avian species, and supervision of poultry movement from affected regions. In addition, regular serosurveys of high-risk personnel (e.g., live poultry markets workers) as well as the general public

TABLE 7 Reference viruses representing each subclade on the HA phylogenetic tree

GISAID accession no.	Isolate name	Subclade
EPI447598	A/Shanghai/05/2013	W1
EPI447629	A/Anhui/02/2013	W1
EPI447614	A/Zhejiang/02/2013	W1
EPI439507	A/Anhui/1/2013	W1
EPI447599	A/Shanghai/07/2013	W1
EPI447596	A/Jiangsu/01/2013	W1
EPI627705	A/Guangdong-Guangzhou/XN08763/2014	W2-1
EPI628512	A/Guangdong/24999/2013	W2-1
EPI627649	A/Guangdong-Guangzhou/XN08423/2014	W2-1
EPI627745	A/Guangdong/0010/2014	W2-1
EPI628520	A/Guangdong/24997/2013	W2-1
EPI628096	A/Guangdong/0012/2014	W2-1
EPI628440	A/Environment/Guangdong/02621/2013	W2-1
EPI627928	A/Fujian/15/2014	W2-2
EPI628056	A/Jiangsu/09387/2014	W2-2
EPI628032	A/Anhui/09186/2014	W2-2
EPI628248	A/Jiangsu/09041/2014	W2-3
EPI627593	A/Zhejiang/13/2014	W2-3
EPI576623	A/Environment/Shanghai/PD-JZ-01/2014	W2-3
EPI627808	A/Shandong/01/2014	W2-4
EPI627537	A/Zhejiang/23/2014	W2-4
EPI627808	A/Shandong/01/2014	W2-4
EPI552399	A/Zhejiang/17/2014	W2-4
EPI628312	A/Zhejiang/07803/2014	W2-4
EPI627441	A/Anhui/01887/2014	W2-5
EPI627912	A/Environment/Xinjiang/73033/2014	W2-5
EPI628416	A/Environment/Jiangsu/03137/2013	W2-5
EPI628224	A/Fujian/6/2014	W2-6
EPI628272	A/Fujian/3/2014	W2-6
EPI628160	A/Fujian/13/2014	W2-6
EPI566044	A/Guangdong/15SF010/2015	W3-1
EPI628712	A/Environment/Guangdong/22351/2015	W3-1
EPI627489	A/Fujian/19/2014	W3-1
EPI559417	A/Hong Kong/2550/2015	W3-1
EPI566036	A/Guangdong/15SF018/2015	W3-1
EPI627209	A/Guangdong/15SF002/2015	W3-2
EPI628648	A/Environment/Guangdong/21123/2015	W3-2
EPI627057	A/Guangdong/15SF051/2015	W3-2
EPI628728	A/Anhui/33228/2015	W3-3
EPI627385	A/Guangdong/02497/2014	W3-3
EPI627097	A/Jiangsu/19758/2015	W3-3
EPI628568	A/Anhui/40095/2015	W3-3
EPI627017	A/Jiangsu/18828/2014	W3-3
EPI628544	A/Beijing/40610/2015	W3-3
EPI566052	A/Xinjiang/05916/2014	W3-3

could be conducted to monitor in a timely fashion potential infections in humans.

ACKNOWLEDGMENTS

This study was supported by the National Mega-projects for Infectious Diseases (2014ZX10004002 and 2013ZX10004218-004, to Y. Shu).

We acknowledge the authors and laboratories for sharing the H7N9 sequences in GISAID's EpiFlu Database. The contents of this article are solely the responsibility of the authors and do not necessarily represent the views of China CDC and other organizations.

REFERENCES

1. **Gao R, Cao B, Hu Y, Feng Z, Wang D, Hu W, Chen J, Jie Z, Qiu H, Xu K, Xu X, Lu H, Zhu W, Gao Z, Xiang N, Shen Y, He Z, Gu Y, Zhang Z, Yang Y, Zhao X, Zhou L, Li X, Zou S, Zhang Y, Li X, Yang L, Guo J, Dong J, Li Q, Dong L, Zhu Y, Bai T, Wang S, Hao P, Yang W, Zhang Y, Han J, Yu H, Li D, Gao GF, Wu G, Wang Y, Yuan Z, Shu Y.** 2013. Human infection with a novel avian-origin influenza A (H7N9) virus. N Engl J Med **368:**1888–1897. http://dx.doi.org/10.1056/NEJMoa1304459.
2. **Zhu W, Shu Y.** 2015. Genetic tuning of avian influenza A (H7N9) virus promotes viral fitness within different species. Microbes Infect **17:**118–122. http://dx.doi.org/10.1016/j.micinf.2014.11.010.
3. **Wu A, Su C, Wang D, Peng Y, Liu M, Hua S, Li T, Gao GF, Tang H, Chen J, Liu X, Shu Y, Peng D, Jiang T.** 2013. Sequential reassortments underlie diverse influenza H7N9 genotypes in China. Cell Host Microbe **14:**446–452. http://dx.doi.org/10.1016/j.chom.2013.09.001.
4. **Wang D, Yang L, Gao R, Zhang X, Tan Y, Wu A, Zhu W, Zhou J, Zou S, Li X, Sun Y, Zhang Y, Liu Y, Liu T, Xiong Y, Xu J, Chen L, Weng Y, Qi X, Guo J, Li X, Dong J, Huang W, Zhang Y, Dong L, Zhao X, Liu L, Lu J, Lan Y, Wei H, Xin L, Chen Y, Xu C, Chen T, Zhu Y, Jiang T, Feng Z, Yang W, Wang Y, Zhu H, Guan Y, Gao GF, Li D, Han J, Wang S, Wu G, Shu Y.** 2014. Genetic tuning of the novel avian influenza A(H7N9) virus during interspecies transmission, China, 2013. Euro Surveill http://www.eurosurveillance.org/ViewArticle.aspx?ArticleId=20836.
5. **Lam TT, Zhou B, Wang J, Chai Y, Shen Y, Chen X, Ma C, Hong W, Chen Y, Zhang Y, Duan L, Chen P, Jiang J, Zhang Y, Li L, Poon LL, Webby RJ, Smith DK, Leung GM, Peiris JS, Holmes EC, Guan Y, Zhu H.** 2015. Dissemination, divergence and establishment of H7N9 influenza viruses in China. Nature **522:**102–105. http://dx.doi.org/10.1038/nature14348.
6. **Lam TT, Wang J, Shen Y, Zhou B, Duan L, Cheung CL, Ma C, Lycett SJ, Leung CY, Chen X, Li L, Hong W, Chai Y, Zhou L, Liang H, Ou Z, Liu Y, Farooqui A, Kelvin DJ, Poon LL, Smith DK, Pybus OG, Leung GM, Shu Y, Webster RG, Webby RJ, Peiris JS, Rambaut A, Zhu H, Guan Y.** 2013. The genesis and source of the H7N9 influenza viruses causing human infections in China. Nature **502:**241–244. http://dx.doi.org/10.1038/nature12515.
7. **Zhang L, Zhang Z, Weng Z.** 2013. Rapid reassortment of internal genes in avian influenza A(H7N9) virus. Clin Infect Dis **57:**1059–1061. http://dx.doi.org/10.1093/cid/cit414.
8. **Cui L, Liu D, Shi W, Pan J, Qi X, Li X, Guo X, Zhou M, Li W, Li J, Haywood J, Xiao H, Yu X, Pu X, Wu Y, Yu H, Zhao K, Zhu Y, Wu B, Jin T, Shi Z, Tang F, Zhu F, Sun Q, Wu L, Yang R, Yan J, Lei F, Zhu B, Liu W, Ma J, Wang H, Gao GF.** 2014. Dynamic reassortments and genetic heterogeneity of the human-infecting influenza A (H7N9) virus. Nat Commun **5:**3142. http://dx.doi.org/10.1038/ncomms4142.
9. **Stamatakis A.** 2014. RAxML version 8: a tool for phylogenetic analysis and post-analysis of large phylogenies. Bioinformatics **30:**1312–1313. http://dx.doi.org/10.1093/bioinformatics/btu033.
10. **Miller MA, Pfeiffer W, Schwartz T.** 2010. Creating the CIPRES Science Gateway for inference of large phylogenetic trees, p 1–8. *In* Proceedings of the Gateway Computing Environments Workshop (GCE), 14 November 2010, New Orleans, LA.
11. **Lu J, Wu J, Zeng X, Guan D, Zou L, Yi L, Liang L, Ni H, Kang M, Zhang X, Zhong H, He X, Monagin C, Lin J, Ke C.** 2014. Continuing reassortment leads to the genetic diversity of influenza virus H7N9 in Guangdong, China. J Virol **88:**8297–8306. http://dx.doi.org/10.1128/JVI.00630-14.
12. **Yang ZF, He JF, Li XB, Guan WD, Ke CW, Wu SG, Pan SH, Li RF, Kang M, Wu J, Lin JY, Ding GY, Huang JC, Pan WQ, Zhou R, Lin YP, Chen RC, Li YM, Chen L, Xiao WL, Zhang YH, Zhong NS.** 2014. Epidemiological and viral genome characteristics of the first human H7N9 influenza infection in Guangdong Province, China. J Thorac Dis **6:**1785–1793. http://dx.doi.org/10.3978/j.issn.2072-1439.2014.12.09.
13. **Shi Y, Zhang W, Wang F, Qi J, Wu Y, Song H, Gao F, Bi Y, Zhang Y, Fan Z, Qin C, Sun H, Liu J, Haywood J, Liu W, Gong W, Wang D, Shu Y, Wang Y, Yan J, Gao GF.** 2013. Structures and receptor binding of hemagglutinins from human-infecting H7N9 influenza viruses. Science **342:**243–247. http://dx.doi.org/10.1126/science.1242917.
14. **Tharakaraman K, Jayaraman A, Raman R, Viswanathan K, Stebbins NW, Johnson D, Shriver Z, Sasisekharan V, Sasisekharan R.** 2013. Glycan receptor binding of the influenza A virus H7N9 hemagglutinin. Cell **153:**1486–1493. http://dx.doi.org/10.1016/j.cell.2013.05.034.
15. **Xiong X, Martin SR, Haire LF, Wharton SA, Daniels RS, Bennett MS, McCauley JW, Collins PJ, Walker PA, Skehel JJ, Gamblin SJ.** 2013.

Receptor binding by an H7N9 influenza virus from humans. Nature **499:** 496–499. http://dx.doi.org/10.1038/nature12372.

16. **Zhou J, Wang D, Gao R, Zhao B, Song J, Qi X, Zhang Y, Shi Y, Yang L, Zhu W, Bai T, Qin K, Lan Y, Zou S, Guo J, Dong J, Dong L, Zhang Y, Wei H, Li X, Lu J, Liu L, Zhao X, Li X, Huang W, Wen L, Bo H, Xin L, Chen Y, Xu C, Pei Y, Yang Y, Zhang X, Wang S, Feng Z, Han J, Yang W, Gao GF, Wu G, Li D, Wang Y, Shu Y.** 2013. Biological features of novel avian influenza A (H7N9) virus. Nature **499:**500–503. http://dx.doi.org/10.1038/nature12379.
17. **Zhang H, Li X, Guo J, Li L, Chang C, Li Y, Bian C, Xu K, Chen H, Sun B.** 2014. The PB2 E627K mutation contributes to the high polymerase activity and enhanced replication of H7N9 influenza virus. J Gen Virol **95:**779–786. http://dx.doi.org/10.1099/vir.0.061721-0.
18. **Mok CK, Lee HH, Lestra M, Nicholls JM, Chan MC, Sia SF, Zhu H, Poon LL, Guan Y, Peiris JS.** 2014. Amino acid substitutions in polymerase basic protein 2 gene contribute to the pathogenicity of the novel A/H7N9 influenza virus in mammalian hosts. J Virol **88:**3568–3576. http://dx.doi.org/10.1128/JVI.02740-13.
19. **Zhu W, Li L, Yan Z, Gan T, Li L, Chen R, Chen R, Zheng Z, Hong W, Wang J, Smith DK, Guan Y, Zhu H, Shu Y.** 2015. Dual E627K and D701N mutations in the PB2 protein of A(H7N9) influenza virus increased its virulence in mammalian models. Sci Rep **5:**14170. http://dx.doi.org/10.1038/srep14170.
20. **Herfst S, Schrauwen EJ, Linster M, Chutinimitkul S, de Wit E, Munster VJ, Sorrell EM, Bestebroer TM, Burke DF, Smith DJ, Rimmelzwaan GF, Osterhaus AD, Fouchier RA.** 2012. Airborne transmission of influenza A/H5N1 virus between ferrets. Science **336:**1534–1541. http://dx.doi.org/10.1126/science.1213362.
21. **Song MS, Marathe BM, Kumar G, Wong SS, Rubrum A, Zanin M, Choi YK, Webster RG, Govorkova EA, Webby RJ.** 2015. Unique determinants of neuraminidase inhibitor resistance among N3, N7, and N9 avian influenza viruses. J Virol **89:**10891–10900. http://dx.doi.org/10.1128/JVI.01514-15.
22. **Chen Y, Liang W, Yang S, Wu N, Gao H, Sheng J, Yao H, Wo J, Fang Q, Cui D, Li Y, Yao X, Zhang Y, Wu H, Zheng S, Diao H, Xia S, Zhang Y, Chan KH, Tsoi HW, Teng JL, Song W, Wang P, Lau SY, Zheng M, Chan JF, To KK, Chen H, Li L, Yuen KY.** 2013. Human infections with the emerging avian influenza A H7N9 virus from wet market poultry: clinical analysis and characterisation of viral genome. Lancet **381:**1916–1925. http://dx.doi.org/10.1016/S0140-6736(13)60903-4.
23. **Kendal APSJ, Pereira MS.** 1982. World Health Organization Collaborating Centers from Reference and Research on Influenza: concepts and procedures for laboratory-based influenza surveillance, p B17–B35. World Health Organization, Geneva, Switzerland.
24. **WHO.** WHO/CDS/CSR/NCS/2002.5. http://www.wpro.who.int/NR/rdonlyres/EFD2B9A7-2265-4AD0-BC98-97937B4FA83C/0/manualonanimalaidiagnosisandsurveillance.pdf. Accessed 21 April 2009.
25. **Pantin-Jackwood MJ, Miller PJ, Spackman E, Swayne DE, Susta L, Costa-Hurtado M, Suarez DL.** 2014. Role of poultry in the spread of novel H7N9 influenza virus in China. J Virol **88:**5381–5390. http://dx.doi.org/10.1128/JVI.03689-13.
26. **Zaraket H, Baranovich T, Kaplan BS, Carter R, Song MS, Paulson JC, Rehg JE, Bahl J, Crumpton JC, Seiler J, Edmonson M, Wu G, Karlsson E, Fabrizio T, Zhu H, Guan Y, Husain M, Schultz-Cherry S, Krauss S, McBride R, Webster RG, Govorkova EA, Zhang J, Russell CJ, Webby RJ.** 2015. Mammalian adaptation of influenza A(H7N9) virus is limited by a narrow genetic bottleneck. Nat Commun **6:**6553. http://dx.doi.org/10.1038/ncomms7553.
27. **Kalthoff D, Bogs J, Grund C, Tauscher K, Teifke JP, Starick E, Harder T, Beer M.** 2014. Avian influenza H7N9/13 and H7N7/13: a comparative virulence study in chickens, pigeons, and ferrets. J Virol **88:**9153–9165. http://dx.doi.org/10.1128/JVI.01241-14.
28. **Gilbert M, Golding N, Zhou H, Wint GR, Robinson TP, Tatem AJ, Lai S, Zhou S, Jiang H, Guo D, Huang Z, Messina JP, Xiao X, Linard C, Van Boeckel TP, Martin V, Bhatt S, Gething PW, Farrar JJ, Hay SI, Yu H.** 2014. Predicting the risk of avian influenza A H7N9 infection in live-poultry markets across Asia. Nat Commun **5:**4116. http://dx.doi.org/10.1038/ncomms5116.
29. **Duan L, Zhu H, Wang J, Huang K, Cheung CL, Peiris JS, Chen H, Guan Y.** 2011. Influenza virus surveillance in migratory ducks and sentinel ducks at Poyang Lake, China. Influenza Other Respir Viruses **5**(Suppl 1)**:**65–68.
30. **Martin V, Pfeiffer DU, Zhou X, Xiao X, Prosser DJ, Guo F, Gilbert M.** 2011. Spatial distribution and risk factors of highly pathogenic avian influenza (HPAI) H5N1 in China. PLoS Pathog **7:**e1001308. http://dx.doi.org/10.1371/journal.ppat.1001308.
31. **Yu X, Jin T, Cui Y, Pu X, Li J, Xu J, Liu G, Jia H, Liu D, Song S, Yu Y, Xie L, Huang R, Ding H, Kou Y, Zhou Y, Wang Y, Xu X, Yin Y, Wang J, Guo C, Yang X, Hu L, Wu X, Wang H, Liu J, Zhao G, Zhou J, Pan J, Gao GF, Yang R, Wang J.** 2014. Influenza H7N9 and H9N2 viruses: coexistence in poultry linked to human H7N9 infection and genome characteristics. J Virol **88:**3423–3431. http://dx.doi.org/10.1128/JVI.02059-13.
32. **Xie S, Jia W, Lin Y, Xing K, Ren X, Qi W, Liao M.** 2015. Third wave of influenza A(H7N9) virus from poultry, Guangdong Province, China, 2014-2015. Emerg Infect Dis **21:**1657–1660. http://dx.doi.org/10.3201/eid2109.150635.